

# Cu(I) Reducibility Controls Ethylene vs Ethanol Selectivity on (100)-Textured Copper during Pulsed CO<sub>2</sub> Reduction

Zhichu Tang, Emily Nishiwaki, Kevin E. Fritz, Tobias Hanrath, and Jin Suntivich\*



Cite This: *ACS Appl. Mater. Interfaces* 2021, 13, 14050–14055



Read Online

## ACCESS |

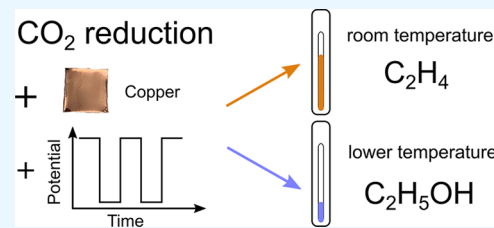
Metrics & More

Article Recommendations

Supporting Information

**ABSTRACT:** The electrochemical CO<sub>2</sub> reduction reaction (CO<sub>2</sub>RR) can convert widely available CO<sub>2</sub> into value-added C<sub>2</sub> products, such as ethylene and ethanol. However, low selectivity toward either compound limits the effectiveness of current CO<sub>2</sub>RR electrocatalysts. Here, we report the use of pulsed overpotentials to improve the ethylene selectivity to 67% with >75% overall C<sub>2</sub> selectivity on (100)-textured polycrystalline Cu foil. The pulsed CO<sub>2</sub>RR can be made selective to either ethylene or ethanol by controlling the reaction temperature. We attribute the enhanced C<sub>2</sub> selectivity to the improved CO dimerization kinetics on the active Cu surface on predominately (100)-textured Cu grains with the reduced hydrogen adsorption coverage during the pulsed CO<sub>2</sub>RR. The ethylene vs ethanol selectivity can be explained by the reducibility of the Cu(I) species during the cathodic potential cycle. Our work demonstrates a simple route to improve the ethylene vs ethanol selectivity and identifies Cu(I) as the species responsible for ethanol production.

**KEYWORDS:** electrochemical CO<sub>2</sub> reduction, pulsed potential, temperature, ethylene, ethanol



## INTRODUCTION

The electrochemical CO<sub>2</sub> reduction reaction (CO<sub>2</sub>RR) has received extensive attention as a solution to the growing demand for sustainably sourced materials and fuels.<sup>1–4</sup> Among the known CO<sub>2</sub>RR catalysts, Cu is unique for its ability to produce hydrocarbons and oxygenates,<sup>5–7</sup> in particular, C<sub>2</sub> products such as ethylene (C<sub>2</sub>H<sub>4</sub>: 2CO<sub>2</sub> + 12H<sup>+</sup> + 12e<sup>−</sup> → C<sub>2</sub>H<sub>4</sub> + 4H<sub>2</sub>O) and ethanol (C<sub>2</sub>H<sub>5</sub>OH: 2CO<sub>2</sub> + 12H<sup>+</sup> + 12e<sup>−</sup> → C<sub>2</sub>H<sub>5</sub>OH + 3H<sub>2</sub>O). As these molecules are the important building blocks for key compounds in the chemical industry, the ability to produce these products by using renewable energy has the potential to sustain the global need for materials and chemicals in the 21st century. However, future progress toward the generation of chemical feedstocks derived from the CO<sub>2</sub>RR remains impaired by the limited selectivity of C<sub>2</sub> products.

Many strategies have been explored to improve the C<sub>2</sub> selectivity of the Cu electrode, to date, including by tuning the Cu surface facet. Hori et al. investigated the structure sensitivity of Cu and found that the (100) facet was more selective to C<sub>2</sub>H<sub>4</sub> (>40%) than the (111) facet (<10%).<sup>8</sup> This selectivity has been attributed to CO<sub>ad</sub> dimerization (the subscript <sub>ad</sub> denotes adsorbed species) on the (100) facet.<sup>9–13</sup> This finding has led to the suggestion that increasing the CO<sub>ad</sub> binding strength on Cu(100)<sup>14</sup> may allow for higher CO<sub>ad</sub> coverage and consequently improved C<sub>2</sub>H<sub>4</sub> selectivity. To this end, strategies for controlling the CO<sub>ad</sub> interaction with Cu surfaces, for example, by controlling facets, morphology, oxidation states, and dopants have been investigated.<sup>15–18</sup> While these methods have yielded a state-of-the-art C<sub>2</sub>

selectivity of >70%, the approaches are often complex and require several synthesis steps. Furthermore, the long-term stability for some of these approaches remains an open challenge.

In comparison to the surface modification methods, the use of pulsed electrochemical potentials has been demonstrated to be a simple and effective way to enhance CO<sub>2</sub>RR selectivity,<sup>19–23</sup> especially to C<sub>2</sub> products.<sup>24</sup> We point out the recent work by Aran-Ais et al., which showed that applying a pulsed potential to Cu(100) single crystals could enhance the C<sub>2</sub>H<sub>5</sub>OH selectivity to 30% and C<sub>2</sub>H<sub>4</sub> to 45%, with >75% combined C<sub>2+</sub> selectivity.<sup>24</sup> This enhancement was attributed to the stabilization of the Cu(I) species which promote C<sub>2</sub>H<sub>5</sub>OH formation without affecting the C<sub>2</sub>H<sub>4</sub> production. While these works have established that the application of a pulsed electrochemical potential can improve the CO<sub>2</sub>RR selectivity over the hydrogen evolution reaction (HER) and support C–C coupling, it is still unclear which factor controls the selectivity between C<sub>2</sub>H<sub>5</sub>OH and C<sub>2</sub>H<sub>4</sub> and whether the enhanced C–C coupling can be directed to only one product such as C<sub>2</sub>H<sub>4</sub>.

In this work, we demonstrate that the factor controlling the selectivity between C<sub>2</sub>H<sub>5</sub>OH and C<sub>2</sub>H<sub>4</sub> is the reduction rate of

Received: October 1, 2020

Accepted: March 2, 2021

Published: March 11, 2021



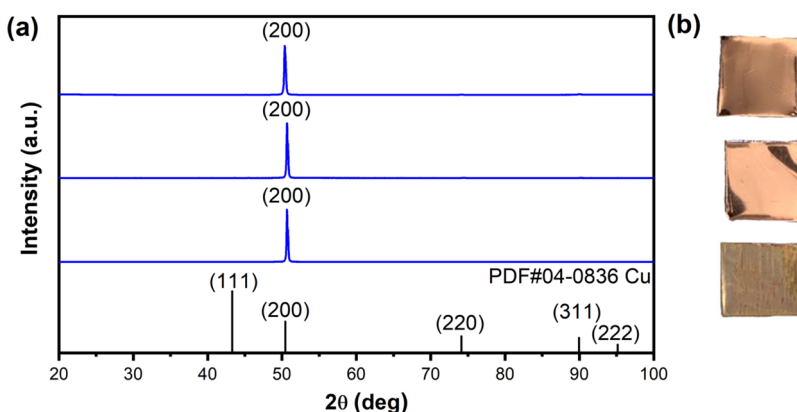


**Figure 1.** (a) XRD patterns (symmetric out-of-plane scan) and (b) corresponding pictures of unreacted Cu foil, Cu foil after 6 h of the constant potential CO<sub>2</sub>RR at -1 V vs RHE, and Cu foil after the 6 h of pulsed potential CO<sub>2</sub>RR at  $E_c = -1$  V vs RHE,  $E_a = 0.6$  V vs RHE, with  $t_a = t_c = 1$  s.

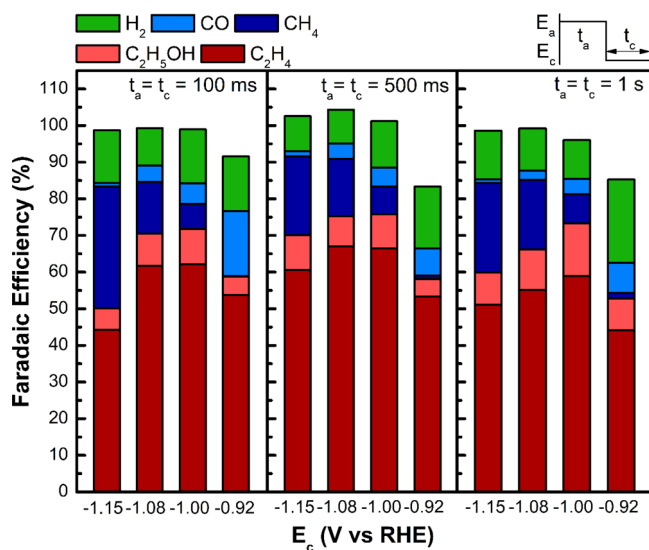
the Cu(I) species during the reduction (cathodic) cycle of the pulsed CO<sub>2</sub>RR. By controlling the reduction kinetics through temperature control, the C<sub>2</sub>H<sub>4</sub> selectivity can be as high as 67% with >75% selectivity toward C<sub>2</sub> products. This C<sub>2</sub> selectivity, which is obtained on a (100)-textured polycrystalline Cu foil under pulsed conditions at 25°C without using any special treatment, is comparable to the state-of-the-art CO<sub>2</sub>RR performance.<sup>17</sup> We hypothesize that the transient species formed during the anodic cycle plays a critical role in the selectivity. Thus, the formation of these transient species can be exploited for selectivity control. We found that by tuning the temperature to control the reduction kinetics, C<sub>2</sub>H<sub>4</sub> can be favored over C<sub>2</sub>H<sub>5</sub>OH. When the reducibility of the surface species formed during the anodic cycle is facile, such as when the cell temperature is held at 25°C, the C<sub>2</sub>H<sub>4</sub> selectivity is enhanced at the expense of C<sub>2</sub>H<sub>5</sub>OH. Along the same line of reasoning, by decreasing the temperature to 15 and 5°C, the active species from the anodic cycle persists during the reduction cycle, positively impacting the C<sub>2</sub>H<sub>5</sub>OH selectivity. The 40% C<sub>2</sub>H<sub>5</sub>OH selectivity at 5°C is among the highest reported in a buffered, neutral electrolyte.<sup>5,24</sup> The finding that the C<sub>2</sub>H<sub>4</sub> vs C<sub>2</sub>H<sub>5</sub>OH competition corresponds proportionally to the response time of the reduction cycle of the pulsed CO<sub>2</sub>RR suggests that the reduction of the surface-oxidized Cu is the factor controlling the C<sub>2</sub> selectivity. Our work has implications on the interpretation of the active species for C<sub>2</sub>H<sub>4</sub> vs C<sub>2</sub>H<sub>5</sub>OH and demonstrates a simple strategy for controlling the selectivity among the C<sub>2</sub> products during the CO<sub>2</sub>RR. The combined use of pulsed electrochemical potentials on Cu foils to improve the C<sub>2</sub> selectivity and controlled temperature to tailor the C<sub>2</sub> selectivity presents a possible strategy for future mechanistic investigations and possibly industrial deployment for selective electrosynthesis.

## RESULTS AND DISCUSSION

We conducted our CO<sub>2</sub>RR experiments in a custom temperature-controlled cell with 0.1 M KHCO<sub>3</sub> electrolyte. X-ray diffraction (XRD) shows that our polycrystalline Cu electrodes consist predominantly of (100) facets (Figure 1), which remain robust throughout the CO<sub>2</sub>RR experiment. We note that this orientation represents a bulk, out-of-plane value and should not be taken to imply that the surface morphology of the polycrystalline foil has a perfect single-crystal-like (100) orientation. Scanning electron microscopy (SEM) showed that the used Cu foil had a rough surface morphology (*vide infra*).

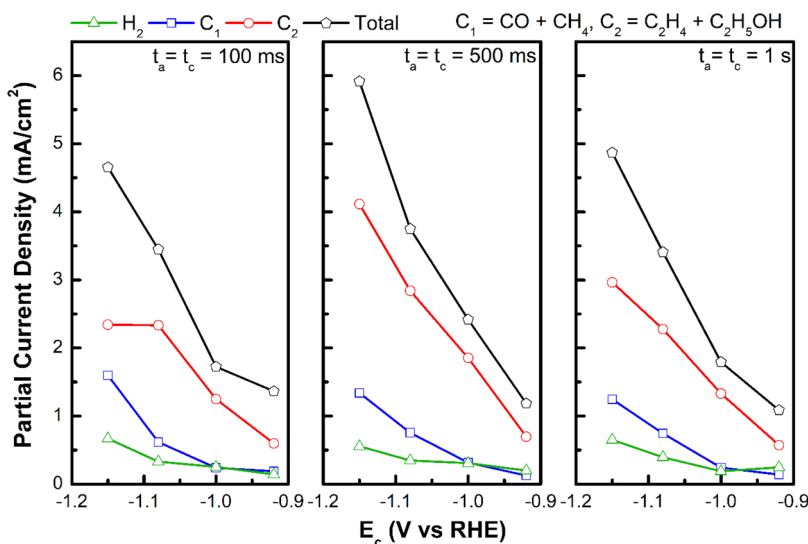
Furthermore, the CO<sub>2</sub>RR under the traditionally used constant electrochemical potential yielded a product distribution (Figure S1) consistent with the literature on polycrystalline Cu.<sup>7,25</sup> We performed the pulsed CO<sub>2</sub>RR using square wave potentials with symmetric anodic and cathodic pulse intervals ( $t_a = t_c$ ). The anodic potential ( $E_a$ ) was set to +0.6 V vs RHE for all measurements, while the cathodic potential ( $E_c$ ) was varied from -0.9 V to -1.15 V vs RHE.

Figure 2 shows the faradaic efficiencies (FEs) of the primary products of the CO<sub>2</sub>RR on Cu for 100 ms, 500 ms, and 1 s



**Figure 2.** Faradaic efficiencies of the main products of the pulsed CO<sub>2</sub>RR on Cu at different  $E_c$  values. All data were collected with  $E_a = 0.6$  V vs RHE and  $t_a = t_c = 100$  ms (left), 500 ms (center), and 1 s (right) at 25°C.

pulsed potentials at 25°C. Similar selectivity trends were observed for all three pulse times, suggesting that the effect of the pulse time was minor. There was a slight enhancement in C<sub>2</sub> selectivity for the 500 ms pulse relative to 100 ms or 1 s pulses (Figure 2). At all potentials, C<sub>2</sub>H<sub>4</sub> was the major product with 50–67% selectivity at most conditions, while CH<sub>4</sub>, H<sub>2</sub>, and CO were suppressed to <20, <15, and <10%, respectively (Figure 2). The C<sub>2</sub>H<sub>5</sub>OH selectivity was ~10%, resulting in the maximum C<sub>2</sub> selectivity >75% at  $E_c = -1$  V vs RHE, with  $t_a = t_c = 500$  ms. This C<sub>2</sub> selectivity corresponds to



**Figure 3.** Partial current densities of  $\text{H}_2$ ,  $\text{C}_1$ , and  $\text{C}_2$  products of the  $\text{CO}_2\text{RR}$  on Cu at different  $E_c$  values, with  $E_a = 0.6$  V vs RHE,  $t_a = t_c = 100$  ms (left), 500 ms (center), and 1 s (right), at 25°C.

a  $\text{C}_2/\text{C}_1$  ratio of  $\sim 5.9$  (Figure S2), much higher than the literature result ( $\sim 1.5$ ) on Cu(100) single crystals under a constant potential.<sup>14</sup> CO production is minimal except at  $E_c = -0.92$  V vs RHE. Interestingly, the total FE also dropped to  $\sim 80$ –90% at this same potential. This observation may reflect the possible CO oxidation during the anodic potential swing.

We analyzed the partial current densities to investigate whether the activity toward  $\text{C}_2$  products was enhanced or the activity toward other products was suppressed (see the Supporting Information for the calculation details). Compared to the previously reported Cu foil with randomly oriented crystal grains,<sup>26</sup> the total  $\text{CO}_2\text{RR}$  current density on (100)-oriented Cu foil was slightly smaller and did not vary significantly with pulse times (Figure 3). However, the partial current density of the  $\text{C}_2$  products at  $-1$  V vs RHE increased by  $2 \times$  (to  $\sim 2$  mA/cm<sup>2</sup> from  $\sim 1$  mA/cm<sup>2</sup>) with respect to the constant potential situation. The partial current densities of the minor products ( $\text{H}_2$  and  $\text{C}_1$ ) decreased to  $\sim 0.6$  mA/cm<sup>2</sup> from  $\sim 3$  mA/cm<sup>2</sup> in the constant potential report.<sup>25</sup> This observation suggests that pulsed potentials both enhance  $\text{C}_2$  generation and suppress other  $\text{CO}_2\text{RR}$  and HER products.

It is important to note that the reported high  $\text{C}_2$  selectivity represents the steady state selectivity, which was attained after  $\sim 2$  h of the measurement. We chose to report the steady-state performance at the end of a 6 h experiment to ensure consistency of the reporting procedure. The change in the  $\text{CO}_2\text{RR}$  FE in the first 2 h, where the  $\text{C}_2\text{H}_4$  FE initially increased, provides information on the origin of the  $\text{C}_2$  selectivity (Figure S3). We observed a coloration of the electrode surface after the pulsed  $\text{CO}_2\text{RR}$  experiment (Figure 1), indicating a cycle of Cu restructuring or redeposition in the first 2 h of the measurement.<sup>27</sup> This finding is consistent with the inductively coupled plasma mass spectrometry (ICP-MS) work by Speck and Cherevko, which found that Cu can dissolve as early as 0.5 V vs RHE.<sup>28</sup> Interestingly, the cyclic voltammogram stayed approximately the same during this period (Figure S4), suggesting minimal changes in surface roughness ( $<20\%$  change in the EDLC response) and adsorption features. We therefore believe that the observed  $\text{C}_2$  selectivity is not due to the increased surface roughness but rather due to the active surface forming over the (100)-

oriented polycrystalline Cu foil. Earlier atomic force microscopy (AFM) investigation on Cu(100) showed that the (100) surface stayed intact during the pulsed  $\text{CO}_2\text{RR}$  through stabilization of the (100) island morphology.<sup>24</sup> Our observation from the cyclic voltammogram showing that the  $\text{CO}_2\text{RR}$  did not significantly change the surface roughness is consistent with the literature's finding. XRD patterns of the polycrystalline Cu foils after a 6 h pulsed potential experiment with  $E_c = -1$  V vs RHE,  $t_a = t_c = 1$  s, as well as a 6 h constant potential experiment with  $E_c = -1$  V vs RHE (Figure 1) show no measurable changes in the facet distribution. We emphasize again that XRD should not be taken as a representative surface model for the Cu foil. SEM shows that the surface Cu foil was rough, even after the  $\text{CO}_2\text{RR}$  (Figure S5). Electron backscatter diffraction (EBSD) showed evidence of (100), (101), and near (112) orientation. However, we were not able to provide a quantitative analysis with the surface roughness of the sample. X-ray photoelectron spectroscopy (XPS) of Cu 2p<sub>3/2</sub> (Figure S6) showed the presence of Cu/Cu<sub>2</sub>O (932.6 eV), CuO (933.6 eV), and Cu(OH)<sub>2</sub> (935.1 eV). Both samples contain a total of  $\sim 20\%$  CuO plus Cu(OH)<sub>2</sub>, similar to the amount of CuO and Cu(OH)<sub>2</sub> observed for unreacted Cu foil in ambient air.<sup>29</sup> Although we cannot resolve Cu vs Cu<sub>2</sub>O due to their overlapping XPS feature, our results suggest that the chemical makeup of the Cu foil did not change going through the constant-potential or pulsed-potential  $\text{CO}_2\text{RR}$ , in agreement with the cyclic voltammogram. Taken together, we hypothesize that the enhanced C–C coupling is due to the active species formed through a series of redox cycles on polycrystalline Cu foil of the preferred (100) orientation. Continuous oxidation and reduction of electrodes under pulsed conditions has been shown to promote the surface  $\text{CO}_{\text{ad}}$  coverage and C–C coupling to ethylene.<sup>27,30,31</sup> This increase in the partial current density of  $\text{C}_2\text{H}_4$  by  $\sim 3 \times$  in the first 2 h of the experiment (Figure S3) agrees with these observations and suggests that the increased C–C coupling is intrinsic to the changing Cu surface chemistry during pulsed potential application instead of the changing surface area.

Reaction temperature is commonly used to tune selectivity. To understand the enhanced  $\text{C}_2\text{H}_4$  selectivity under pulsed conditions, we tested the effect of temperature on the pulsed

CO<sub>2</sub>RR at 5 and 15°C using the same experimental parameters. The activation energy for C<sub>2</sub>H<sub>4</sub> formation under pulsed conditions was calculated to be 25.98 ± 3.88 kJ/mol (Figure S7) at -1 V vs RHE, which is lower than the C<sub>2</sub>H<sub>4</sub> activation energy under constant potential conditions (~35 kJ/mol).<sup>25</sup> This reduced activation energy for C<sub>2</sub>H<sub>4</sub> production supports our hypothesis of enhanced C<sub>2</sub>H<sub>4</sub> production under pulsed conditions. Under constant potential conditions, the C–C coupling process is limited by the low CO<sub>ad</sub> coverage, where CO<sub>ad</sub> must compete against H<sub>ad</sub> for available Cu sites.<sup>32</sup> Under pulsed potential conditions, we hypothesize that a cycle of oxidizing–reducing potential allows H<sub>ad</sub> to preferentially desorb. While CO<sub>ad</sub> can similarly desorb or oxidize at the oxidative potential, we postulate that the kinetics are slower than the H<sub>ad</sub> desorption. The H<sub>ad</sub> desorption creates open Cu sites to allow the CO<sub>ad</sub> coverage to increase relative to H<sub>ad</sub>, favoring C–C coupling.<sup>27</sup> This effect should simultaneously suppress HER, enhance C–C coupling, and minimize the C<sub>1</sub> product formation, which are the results observed under pulsed potentials.

The critical question is why it is that our C<sub>2</sub>H<sub>4</sub> selectivity (>65%) is significantly higher than Aran-Ais et al., whose investigation using a similarly designed experiment showed similar C<sub>2</sub> selectivity (~75%) but with significantly lower C<sub>2</sub>H<sub>4</sub> selectivity (~45%).<sup>24</sup> We postulate that the difference could be because most CO<sub>2</sub>RR experiments are conducted at room temperature that is closer to 20°C, which is lower than the temperature used in our experiment (25°C). To test this hypothesis, we tested the selectivity at 5 and 15°C for a variety of voltages with  $E_a = 0.6$  V and  $t_a = t_c = 1$  s. In agreement with our hypothesis, we observed a significant temperature dependence of the selectivity between C<sub>2</sub>H<sub>4</sub> and C<sub>2</sub>H<sub>5</sub>OH (Figure 4). At 5°C, C<sub>2</sub>H<sub>5</sub>OH selectivity is relatively voltage-

selectivity toward C<sub>2</sub> products remains >60%, with C<sub>2</sub>H<sub>4</sub> and C<sub>2</sub>H<sub>5</sub>OH selectivity at values between the 5 and 25°C experiments. We also note that HER selectivity is suppressed to <15% for all potentials at 5 and 15°C (Figure S8), which further strengthens the argument that pulsed voltages suppress HER by decreasing the coverage of H<sub>ad</sub> on the Cu surface. The amount of formate increases as the overpotential becomes less negative at both temperatures.

Our results demonstrate that the ratio of C<sub>2</sub>H<sub>4</sub> to C<sub>2</sub>H<sub>5</sub>OH is sensitive to reaction temperature, with higher temperatures favoring C<sub>2</sub>H<sub>4</sub> and lower temperatures favoring C<sub>2</sub>H<sub>5</sub>OH. To explain this observation, we consider a shift in the equilibrium between C<sub>2</sub>H<sub>4</sub> and C<sub>2</sub>H<sub>5</sub>OH due to the hydration reaction (C<sub>2</sub>H<sub>4(g)</sub> + H<sub>2</sub>O<sub>(l)</sub> → C<sub>2</sub>H<sub>5</sub>OH<sub>(l)</sub>,  $\Delta G^0 = -6$  kJ/mol).<sup>33</sup> If the observed C<sub>2</sub>H<sub>5</sub>OH selectivity was due to faster C<sub>2</sub>H<sub>4</sub> hydration kinetics at higher temperature, the C<sub>2</sub>H<sub>4</sub> to C<sub>2</sub>H<sub>5</sub>OH ratio should move closer to equilibrium at 25°C. However, we observed the opposite result, indicating that the observed effect is not due to the hydration effect, i.e., the observed C<sub>2</sub>H<sub>4</sub> vs C<sub>2</sub>H<sub>5</sub>OH selectivity is a result of catalysis. Cu single-crystal studies attributed the enhancement in the C<sub>2</sub>H<sub>4</sub> selectivity to the (100) facets<sup>34</sup> and C<sub>2</sub>H<sub>5</sub>OH selectivity to the stabilization of Cu(I) under pulsed conditions.<sup>24</sup> These surface Cu(I) species could create an oxophilic surface that stabilizes the adsorbed oxygen that impacts the branching point between the C<sub>2</sub>H<sub>4</sub> and C<sub>2</sub>H<sub>5</sub>OH pathways, i.e., OHCH<sub>2,ad</sub>.<sup>24</sup> Based on this prior mechanistic proposal, the temperature-dependent C<sub>2</sub>H<sub>4</sub> vs C<sub>2</sub>H<sub>5</sub>OH selectivity observed in our experiments is likely a result of how Cu(I) is stabilized during the pulsed potential, where lower temperature more effectively stabilizes the Cu(I) species.

To understand why Cu(I) is stabilized at lower temperature, we examined the temperature dependence of the current response during the pulsed CO<sub>2</sub>RR (Figure S9). Similar to the previous report,<sup>21</sup> we observe a sharp current spike at the beginning of each pulse which decays to a stable current on the ms timescale. We characterize the response time by fitting an exponential function and extracting the time constant, which we found to increase with decreasing temperature (Figure S10). Specifically, the time constant in the reductive cycle (cathodic pulse) was found to be higher at 5°C than at 25°C. We believe that this result indicates the slow kinetics of the reduction of Cu(I) to Cu(0) at low temperature. The similar oxidation and reduction time constants at 25°C indicate that a smaller fraction of residual Cu(I) stays intact during the reductive cycle. Thus, C<sub>2</sub>H<sub>4</sub> enhancement is a result of the Cu(I) species being reductively eliminated on the Cu(100) facet, while the higher time constants at low temperature kinetically stabilize Cu(I), effectively allowing the Cu(I) species to facilitate the C<sub>2</sub>H<sub>5</sub>OH production as has been previously reported.<sup>24</sup> Based on this mechanism, our C<sub>2</sub>H<sub>4</sub> enhancement at 25°C compared to the previously reported enhancement in C<sub>2</sub>H<sub>5</sub>OH on Cu(100) single crystals at room temperature is due to our active control of the reaction temperature at 25°C vs an uncontrolled system that is likely closer to ~20°C. Most importantly, our analysis suggests that the species responsible for C<sub>2</sub>H<sub>5</sub>OH is Cu(I) while the active sites responsible for C<sub>2</sub>H<sub>4</sub> are the reduced Cu facets. Although both Cu(0) and Cu(I) are capable of supporting C–C coupling, the former favors C<sub>2</sub>H<sub>4</sub> formation while the latter favors C<sub>2</sub>H<sub>5</sub>OH.

The details of the exact atomic structure during cycling and its relationship to the C–C coupling remains an open

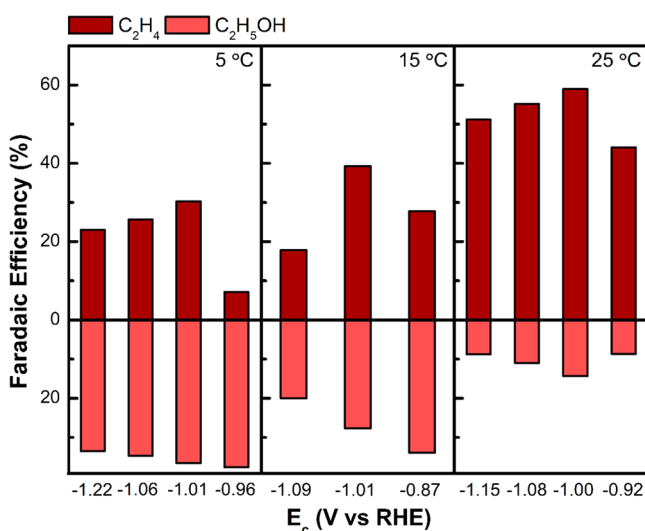


**Figure 4.** Faradaic efficiencies of ethylene and ethanol for the CO<sub>2</sub>RR on Cu at different  $E_c$  values, with  $E_a = 0.6$  V vs RHE,  $t_a = t_c = 1$  s, at 5, 15, and 25°C.

independent with an FE between 30 and 40%, which is among the highest C<sub>2</sub>H<sub>5</sub>OH selectivity reported in an H-cell with neutral bicarbonate electrolyte.<sup>5,24</sup> Combined with C<sub>2</sub>H<sub>4</sub>, the total C<sub>2</sub> selectivity is >60%, which suggests that under pulsed conditions the total C<sub>2</sub> selectivity does not strongly depend on temperature. The results at 15°C support this trend—the

question. Polycrystalline surfaces are complicated by the presence of different terminations and structural defects, including grain boundaries and morphologies. In addition to this issue, it is possible that the oxygen atom near the oxidized Cu can migrate into the subsurface. In such situations, the cathodic pulse may not fully reduce the subsurface oxygen since it is kinetically inaccessible, leading to persistent subsurface oxygen species. Several groups have suggested that subsurface oxygen can enhance  $C_2H_4$  selectivity on Cu by increasing the  $CO_{ad}$  binding energy which enhances C–C coupling.<sup>35,36</sup> Additionally, Cu(I) may be stabilized by  $OH_{ad}$  formed via water electro-oxidation ( $H_2O \rightarrow OH_{ad} + H^+ + e^-$ ), the residue of which could participate in the  $CO_2RR$ . Understanding the nature of the oxidized Cu will be essential in understanding and eventually improving the pulsed  $CO_2RR$  performance in the future.

## CONCLUSIONS

In summary, we report a highly  $C_2H_4$ -selective (67%)  $CO_2RR$  using square wave potentials on (100)-textured polycrystalline Cu foil with >75% total  $C_2$  selectivity. We show that temperature plays a crucial role in whether the  $CO_2RR$  favors ethylene or ethanol with the maximum ethylene production found at 25°C (67%) and the maximum ethanol production found at lower temperature (up to 40%). We attribute the overall enhancement in  $C_2$  selectivity to the reduced  $H_{ad}$  coverage, which enhances the  $CO_{ad}$  coverage to support C–C coupling during the pulsed  $CO_2RR$ . The  $C_2H_4$  selectivity is favored at higher temperature where the cathodic pulse can reduce the majority of Cu(I) to Cu(0). On the other hand, the Cu(I) species persist at a lower temperature, causing the  $CO_2RR$  to favor  $C_2H_5OH$ . Our results establish a simple method for not only enhancing the  $CO_2RR$  selectivity toward the  $C_2$  products but also to tailor the  $C_2H_4:C_2H_5OH$  ratio through controlling the reaction temperature.

## ASSOCIATED CONTENT

### Supporting Information

The Supporting Information is available free of charge at <https://pubs.acs.org/doi/10.1021/acsami.0c17668>.

Experimental methods; FE of main products of the  $CO_2RR$  under constant potentials; the current ratio of  $C_2/C_1$  for the  $CO_2RR$  under pulsed potentials; FE and partial current densities of major products of the  $CO_2RR$  over time; CV of Cu foil in 0.1 M KOH before and after the  $CO_2RR$ ; XPS data of Cu foil before and after the  $CO_2RR$ ; Arrhenius plot of the  $C_2H_4$  partial current density; FE of main products of the  $CO_2RR$  under pulsed potentials at 5 and 15°C; pulsed current for 5, 15, and 25°C; and the time constant of cathodic and anodic pulses ([PDF](#))

## AUTHOR INFORMATION

### Corresponding Author

Jin Suntivich – Department of Materials Science and Engineering, Cornell University, Ithaca, New York 14853, United States; Kavli Institute at Cornell for Nanoscale Science, Cornell University, Ithaca, New York 14853, United States; [orcid.org/0000-0002-3427-4363](https://orcid.org/0000-0002-3427-4363); Email: [jsuntivich@cornell.edu](mailto:jsuntivich@cornell.edu)

## Authors

Zhichu Tang – Department of Materials Science and Engineering, Cornell University, Ithaca, New York 14853, United States

Emily Nishiwaki – Department of Materials Science and Engineering, Cornell University, Ithaca, New York 14853, United States; Department of Chemistry and Chemical Biology, Cornell University, Ithaca, New York 14853, United States; [orcid.org/0000-0002-3419-8604](https://orcid.org/0000-0002-3419-8604)

Kevin E. Fritz – Department of Materials Science and Engineering, Cornell University, Ithaca, New York 14853, United States; [orcid.org/0000-0002-9033-8157](https://orcid.org/0000-0002-9033-8157)

Tobias Hanrath – Robert Frederick Smith School of Chemical and Biomolecular Engineering, Cornell University, Ithaca, New York 14853, United States; [orcid.org/0000-0001-5782-4666](https://orcid.org/0000-0001-5782-4666)

Complete contact information is available at: <https://pubs.acs.org/10.1021/acsami.0c17668>

## Author Contributions

Z.T., E.N., and J.S. conceived the experimental design. Z.T., E.N., and K.E.F. conducted the experiments and analyzed the data. T.H. contributed to the discussion. Z.T. and J.S. prepared the manuscript with help from E.N. and K.E.F. All authors have approved the final version of the manuscript.

## Funding

This work was supported by the National Science Foundation (NSF) under Grant No. CBET-1805400. This work also made use of the Cornell Center for Materials Research Shared Facilities which are supported through the NSF MRSEC program (DMR-1719875).

## Notes

The authors declare no competing financial interest.

## ACKNOWLEDGMENTS

The authors thank Yixu Zong, Kevin Kimura, Abigail Nason, and Don Werder for their help with the temperature-control setup, the faradaic efficiency analysis, and the Cu foil characterization.

## REFERENCES

- (1) De Luna, P.; Hahn, C.; Higgins, D.; Jaffer, S. A.; Jaramillo, T. F.; Sargent, E. H. What would it take for renewably powered electrosynthesis to displace petrochemical processes? *Science* **2019**, 364, No. eaav3506.
- (2) Chen, C.; Kotyk, J. F. K.; Sheehan, S. W. Progress toward Commercial Application of Electrochemical Carbon Dioxide Reduction. *Chem* **2018**, 4, 2571–2586.
- (3) Smith, W. A.; Burdyny, T.; Vermaas, D. A.; Geerlings, H. Pathways to Industrial-Scale Fuel Out of Thin Air from  $CO_2$  Electrolysis. *Joule* **2019**, 3, 1822–1834.
- (4) Whipple, D. T.; Kenis, P. J. A. Prospects of  $CO_2$  Utilization via Direct Heterogeneous Electrochemical Reduction. *J. Phys. Chem. Lett.* **2010**, 1, 3451–3458.
- (5) Nitopi, S.; Bertheussen, E.; Scott, S. B.; Liu, X. Y.; Engstfeld, A. K.; Horch, S.; Seger, B.; Stephens, I. E. L.; Chan, K.; Hahn, C.; Norskov, J. K.; Jaramillo, T. F.; Chorkendorff, I. Progress and Perspectives of Electrochemical  $CO_2$  Reduction on Copper in Aqueous Electrolyte. *Chem. Rev.* **2019**, 119, 7610–7672.
- (6) Li, C. W.; Kanan, M. W.  $CO_2$  Reduction at Low Overpotential on Cu Electrodes Resulting from the Reduction of Thick  $Cu_2O$  Films. *J. Am. Chem. Soc.* **2012**, 134, 7231–7234.

(7) Hori, Y. In *Modern Aspects of Electrochemistry*, No 42 *Modern Aspects of Electrochemistry*, eds Vayenas, C. G.; White, R. E.; GamboaAldeco, M. E.; Springer, 89–189 (2008).

(8) Hori, Y.; Takahashi, I.; Koga, O.; Hoshi, N. Electrochemical reduction of carbon dioxide at various series of copper single crystal electrodes. *J. Mol. Catal. A-Chem.* **2003**, *199*, 39–47.

(9) Montoya, J. H.; Shi, C.; Chan, K.; Norskov, J. K. Theoretical Insights into a CO Dimerization Mechanism in CO<sub>2</sub> Electroreduction. *J. Phys. Chem. Lett.* **2015**, *6*, 2032–2037.

(10) Calle-Vallejo, F.; Koper, M. T. M. Theoretical Considerations on the Electroreduction of CO to C<sub>2</sub> Species on Cu(100) Electrodes. *Angew. Chem.-Int. Edit.* **2013**, *52*, 7282–7285.

(11) Schouten, K. J. P.; Kwon, Y.; Van der Ham, C. J. M.; Qin, Z.; Koper, M. T. M. A new mechanism for the selectivity to C<sub>1</sub> and C<sub>2</sub> species in the electrochemical reduction of carbon dioxide on copper electrodes. *Chem. Sci.* **2011**, *2*, 1902–1909.

(12) Gao, D. F.; Aran-Ais, R. M.; Jeon, H. S.; Roldan Cuenya, B. Rational catalyst and electrolyte design for CO<sub>2</sub> electroreduction towards multicarbon products. *Nat. Catal.* **2019**, *2*, 198–210.

(13) Perez-Gallent, E.; Figueiredo, M. C.; Calle-Vallejo, F.; Koper, M. T. M. Spectroscopic Observation of a Hydrogenated CO Dimer Intermediate During CO Reduction on Cu(100) Electrodes. *Angew. Chem.-Int. Edit.* **2017**, *56*, 3621–3624.

(14) Huang, Y.; Handoko, A. D.; Hirunsit, P.; Yeo, B. S. Electrochemical Reduction of CO<sub>2</sub> Using Copper Single-Crystal Surfaces: Effects of CO\* Coverage on the Selective Formation of Ethylene. *ACS Catal.* **2017**, *7*, 1749–1756.

(15) Li, F. W.; Thevenon, A.; Rosas-Hernández, A.; Wang, Z. Y.; Li, Y. L.; Gabardo, C. M.; Ozden, A.; Dinh, C. T.; Li, J.; Wang, Y. H.; Edwards, J. P.; Xu, Y.; McCallum, C.; Tao, L. Z.; Liang, Z. Q.; Luo, M. C.; Wang, X.; Li, H. H.; O'Brien, C. P.; Tan, C. S.; Nam, D. H.; Quintero-Bermudez, R.; Zhuang, T. T.; Li, Y. G. C.; Han, Z. J.; Britt, R. D.; Sinton, D.; Agapie, T.; Peters, J. C.; Sargent, E. H. Molecular tuning of CO<sub>2</sub>-to-ethylene conversion. *Nature* **2020**, *577*, 509.

(16) Jiang, K.; Sandberg, R. B.; Akey, A. J.; Liu, X. Y.; Bell, D. C.; Norskov, J. K.; Chan, K. R.; Wang, H. T. Metal ion cycling of Cu foil for selective C-C coupling in electrochemical CO<sub>2</sub> reduction. *Nat. Catal.* **2018**, *1*, 111–119.

(17) Zhou, Y. S.; Che, F. L.; Liu, M.; Zou, C. Q.; Liang, Z. Q.; De Luna, P.; Yuan, H. F.; Li, J.; Wang, Z. Q.; Xie, H. P.; Li, H. M.; Chen, P. N.; Bladt, E.; Quintero-Bermudez, R.; Sham, T. K.; Bals, S.; Hofkens, J.; Sinton, D.; Chen, G.; Sargent, E. H. Dopant-induced electron localization drives CO<sub>2</sub> reduction to C<sub>2</sub> hydrocarbons. *Nat. Chem.* **2018**, *10*, 974–980.

(18) Yang, K. D.; Ko, W. R.; Lee, J. H.; Kim, S. J.; Lee, H.; Lee, M. H.; Nam, K. T. Morphology-Directed Selective Production of Ethylene or Ethane from CO<sub>2</sub> on a Cu Mesopore Electrode. *Angew. Chem.-Int. Edit.* **2017**, *56*, 796–800.

(19) Shiratsuchi, R.; Aikoh, Y.; Nogami, G. Pulsed Electroreduction of CO<sub>2</sub> on Copper Electrodes. *J. Electrochem. Soc.* **1993**, *140*, 3479–3482.

(20) Kumar, B.; Brian, J. P.; Atla, V.; Kumari, S.; Bertram, K. A.; White, R. T.; Spurgeon, J. M. Controlling the Product Syngas H<sub>2</sub>:CO Ratio through Pulsed-Bias Electrochemical Reduction of CO<sub>2</sub> on Copper. *ACS Catal.* **2016**, *6*, 4739–4745.

(21) Kimura, K. W.; Fritz, K. E.; Kim, J.; Suntivich, J.; Abruna, H. D.; Hanrath, T. Controlled Selectivity of CO<sub>2</sub> Reduction on Copper by Pulsing the Electrochemical Potential. *ChemSusChem* **2018**, *11*, 1781–1786.

(22) Engelbrecht, A.; Uhlig, C.; Stark, O.; Hammerle, M.; Schmid, G.; Magori, E.; Wiesner-Fleischer, K.; Fleischer, M.; Moos, R. On the Electrochemical CO<sub>2</sub> Reduction at Copper Sheet Electrodes with Enhanced Long-Term Stability by Pulsed Electrolysis. *J. Electrochem. Soc.* **2018**, *165*, J3059–J3068.

(23) Yano, J.; Morita, T.; Shimano, K.; Nagami, Y.; Yamasaki, S. Selective ethylene formation by pulse-mode electrochemical reduction of carbon dioxide using copper and copper-oxide electrodes. *J. Solid State Electrochem.* **2007**, *11*, 554–557.

(24) Aran-Ais, R. M.; Scholten, F.; Kunze, S.; Rizo, R.; Cuenya, B. R. The role of in situ generated morphological motifs and Cu(I) species in C<sub>2+</sub> product selectivity during CO<sub>2</sub> pulsed electroreduction. *Nat. Energy* **2020**, *5*, 317–325.

(25) Zong, Y.; Chakthranont, P.; Suntivich, J. Temperature Effect of CO<sub>2</sub> Reduction Electrocatalysis on Copper: Potential Dependency of Activation Energy. *J. Electrochem. En. Conv. Stor.* **2020**, *17*, No. 041105.

(26) Kuhl, K. P.; Cave, E. R.; Abram, D. N.; Jaramillo, T. F. New insights into the electrochemical reduction of carbon dioxide on metallic copper surfaces. *Energy Environ. Sci.* **2012**, *5*, 7050–7059.

(27) Kimura, K. W.; Casebolt, R.; Cimada DaSilva, J.; Kauffman, E.; Kim, J.; Dunbar, T. A.; Pollock, C. J.; Suntivich, J.; Hanrath, T. Selective Electrochemical CO<sub>2</sub> Reduction during Pulsed Potential Stems from Dynamic Interface. *ACS Catal.* **2020**, *10*, 8632–8639.

(28) Speck, F. D.; Cherevko, S. Electrochemical copper dissolution: A benchmark for stable CO<sub>2</sub> reduction on copper electrocatalysts. *Electrochem. Commun.* **2020**, *115*, No. 106739.

(29) Platzman, I.; Brener, R.; Haick, H.; Tannenbaum, R. Oxidation of polycrystalline copper thin films at ambient conditions. *J. Phys. Chem. C* **2008**, *112*, 1101–1108.

(30) Hori, Y.; Murata, A.; Takahashi, R. Formation of hydrocarbons in the electrochemical reduction of carbon dioxide at a copper electrode in aqueous solution. *J. Chem. Soc., Faraday Trans.* **1989**, *85*, 2309–2326.

(31) Jiang, K.; Huang, Y. F.; Zeng, G. S.; Toma, F. M.; Goddard, W. A.; Bell, A. T. Effects of Surface Roughness on the Electrochemical Reduction of CO<sub>2</sub> over Cu. *ACS Energy Lett.* **2020**, *5*, 1206–1214.

(32) Kortlever, R.; Shen, J.; Schouten, K. J. P.; Calle-Vallejo, F.; Koper, M. T. M. Catalysts and Reaction Pathways for the Electrochemical Reduction of Carbon Dioxide. *J. Phys. Chem. Lett.* **2015**, *6*, 4073–4082.

(33) In *CRC Handbook of Chemistry and Physics*, 101st Edition Rumble, J. R. CRC Press/Taylor & Francis, 2020.

(34) Schouten, K. J. P.; Qin, Z. S.; Gallent, E. P.; Koper, M. T. M. Two Pathways for the Formation of Ethylene in CO Reduction on Single-Crystal Copper Electrodes. *J. Am. Chem. Soc.* **2012**, *134*, 9864–9867.

(35) Favaro, M.; Xiao, H.; Cheng, T.; Goddard, W. A.; Yano, J.; Crumlin, E. J. Subsurface oxide plays a critical role in CO<sub>2</sub> activation by Cu(111) surfaces to form chemisorbed CO<sub>2</sub>, the first step in reduction of CO<sub>2</sub>. *Proc. Natl. Acad. Sci. U. S. A.* **2017**, *114*, 6706–6711.

(36) Eilert, A.; Cavalca, F.; Roberts, F. S.; Osterwalder, J.; Liu, C.; Favaro, M.; Crumlin, E. J.; Ogasawara, H.; Friebel, D.; Pettersson, L. G. M.; Nilsson, A. Subsurface Oxygen in Oxide-Derived Copper Electrocatalysts for Carbon Dioxide Reduction. *J. Phys. Chem. Lett.* **2016**, *8*, 285–290.